

Supporting Information

Quantitating Cell-Cell Interaction Functions, with Applications to Glioblastoma Multiforme Cancer Cells

Jun Wang[†], Douglas Tham[†], Wei Wei[†], Young Shik Shin[†], Chao Ma[†], Habib Ahmad[†], Qihui Shi[†], Jenkan Yu[†], Raphael D. Levine^{#,‡}, and James R. Heath^{†,*}

[†]NanoSystems Biology Cancer Center, Division of Chemistry and Chemical Engineering, Caltech, Pasadena CA 91125.

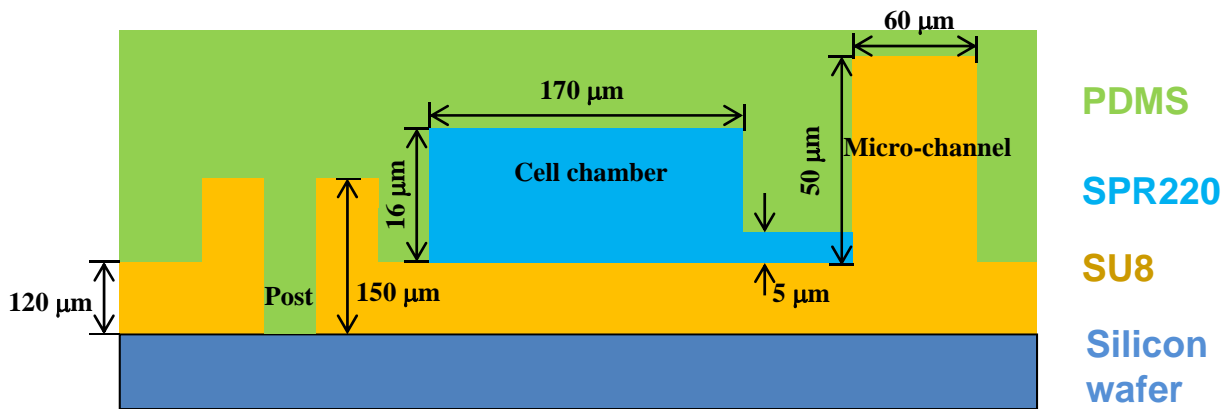
[#]The Fritz Haber Research Center for Molecular Dynamics, The Institute of Chemistry, The Hebrew University of Jerusalem, Jerusalem 91904, Israel.

[‡]Crump Institute for Molecular Imaging, Department of Molecular and Medical Pharmacology, UCLA, Los Angeles, CA 90095.

*Correspondence to: heath@caltech.edu

1. Supporting Figures S1 – S11	1-11
2. Supporting Tables S1 – S3	12-14
3. Supporting Materials and Methods	15-19

a.



b.

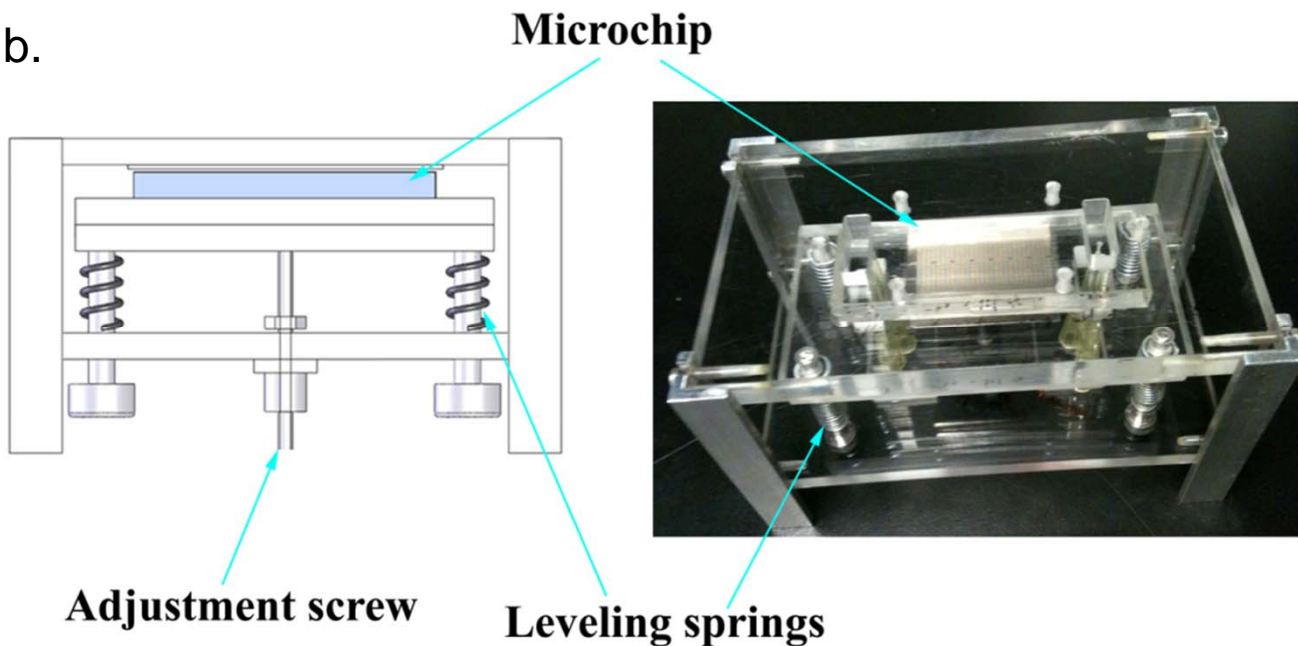


Figure S1. Design and operational components of the valveless SCBC design. a. The three dimensional mold for the elastomeric (PDMS) microfluidics layer, shown in side-view cross section. The drawing is not to scale, so as to illustrate some of the important features. SU8 and SPR220 are photoresist materials that are patterned through a series of masking/photolithography steps to produce the structure shown. b. The clamp system used to partially (Close I state) or fully close (Close II state), or hold open the conduits between the microchannels and the cell chamber.

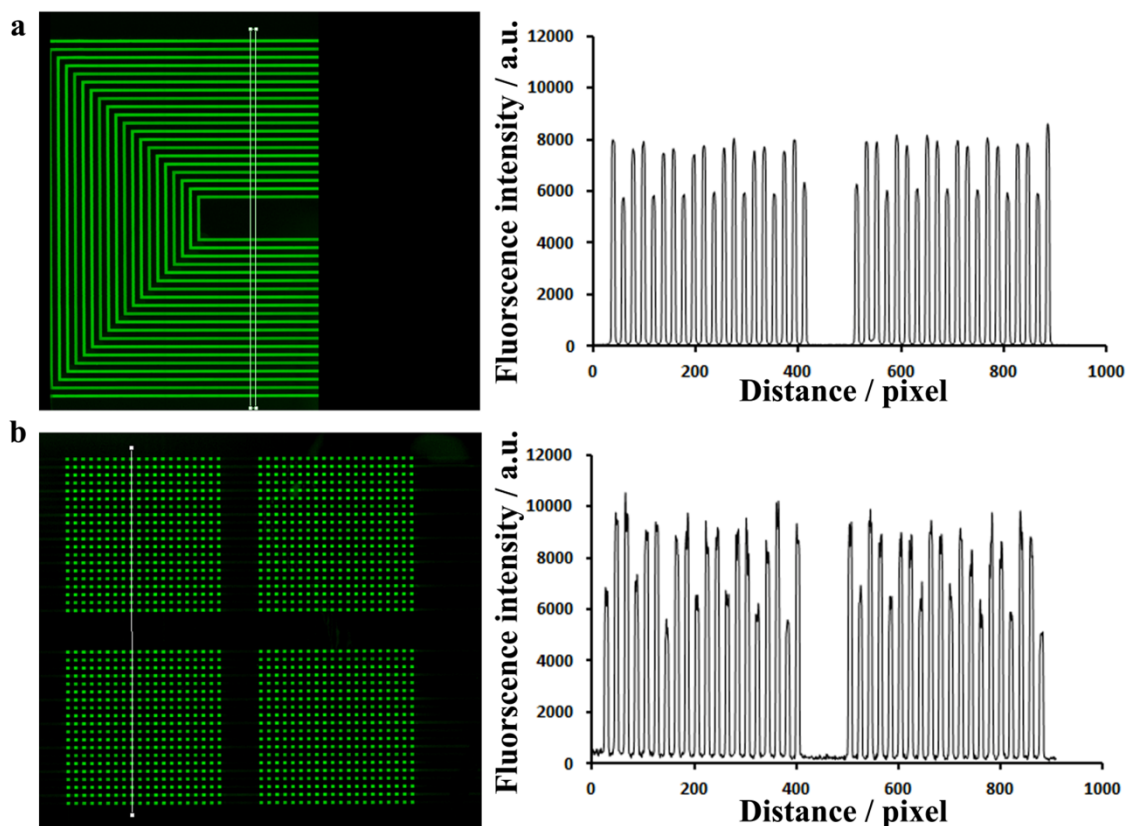


Figure S2. Reproducibility of the ssDNA array. (a) Validation of the first layer of ssDNA array. The plot in the right shows the intensity of each stripe in the left figure, along the drawn vertical line. 3 different ssDNA sequences were repetitively patterned in 20 channels. (b) Validation of the barcode array after the second flow patterning step. Each square unit of fluorescent spots represents many copies of a 3x3 array. The plot at right provides the fluorescence intensity of the vertical line that is drawn through 2 of the square units.

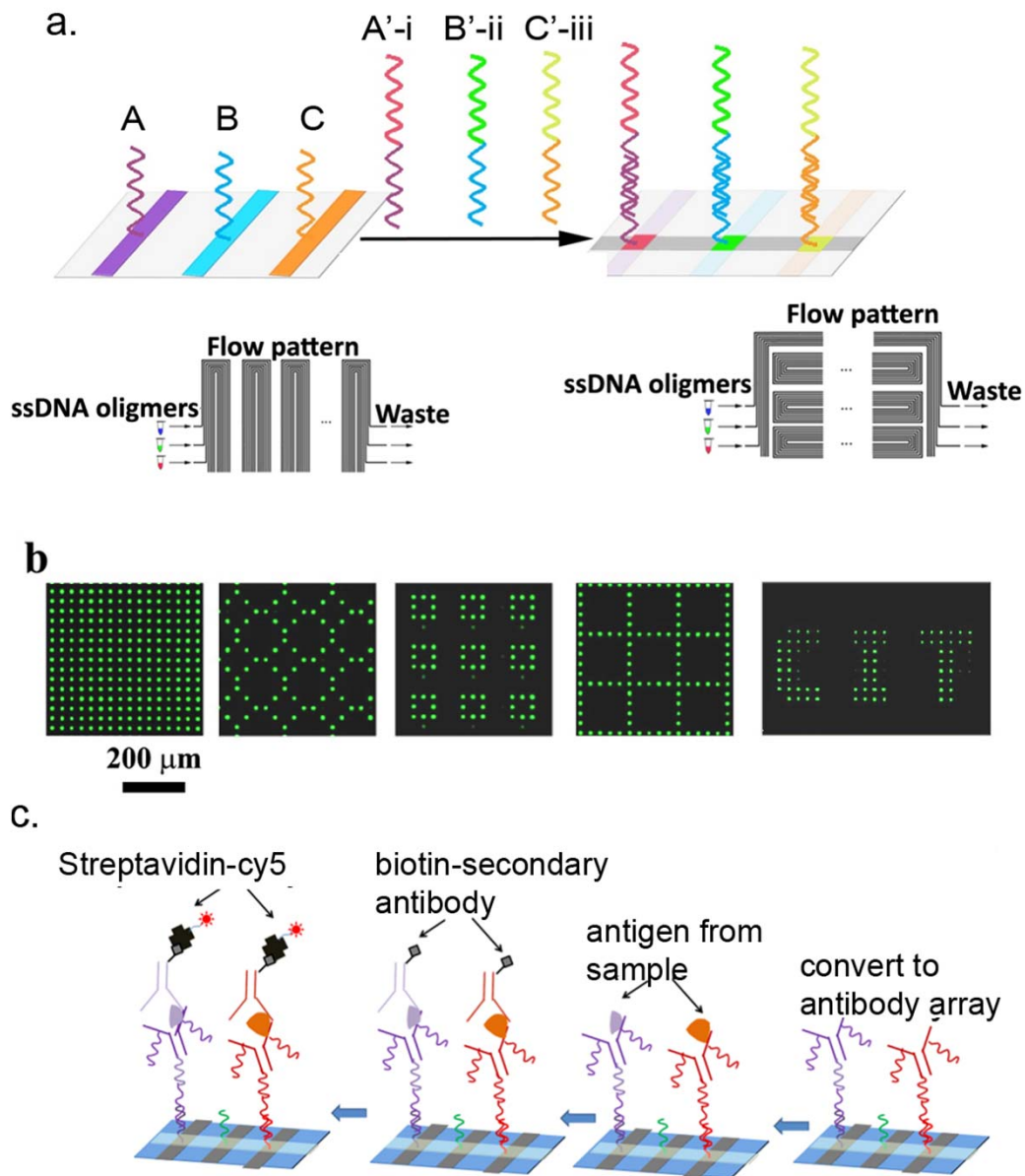


Figure S3. The antibody microarray construction. (a) Schematic illustration of the chemical patterning steps to produce the high-density ssDNA array. Stripes of DNA are first patterned onto a polylysine-coated glass surface using a flow patterning mold oriented as shown in the lower left drawing of a. A second similar flow patterning step, but oriented perpendicular to the first, is used to create unique DNA addresses at the intersections of the crossed stripes. The color coded DNA oligomers in the drawing illustrate the patterning/hybridization sequence to produce the final array. (b) The addressability of the individual spots within each array is illustrated in these images of different DNA patterns prepared as shown in (a). In each case, a uniform, square array is patterned, but with unique DNA addresses at the different array spots. Selective addition of a set of Cy3-complementary DNA oligomers is done to highlight that the flexibility of this patterning approach. (c) The steps of the sandwich ELISA-like assay that is utilized for protein detection³ once the DNA array has been converted into an antibody array.

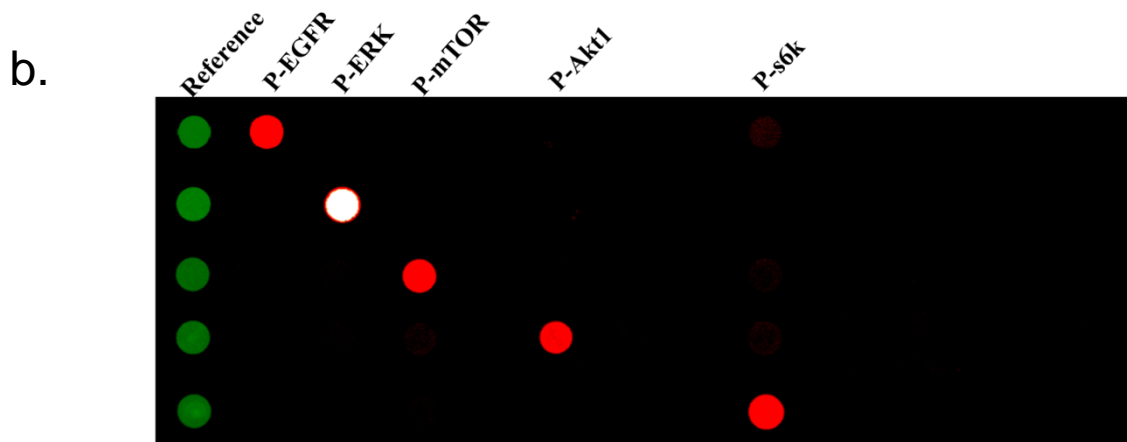
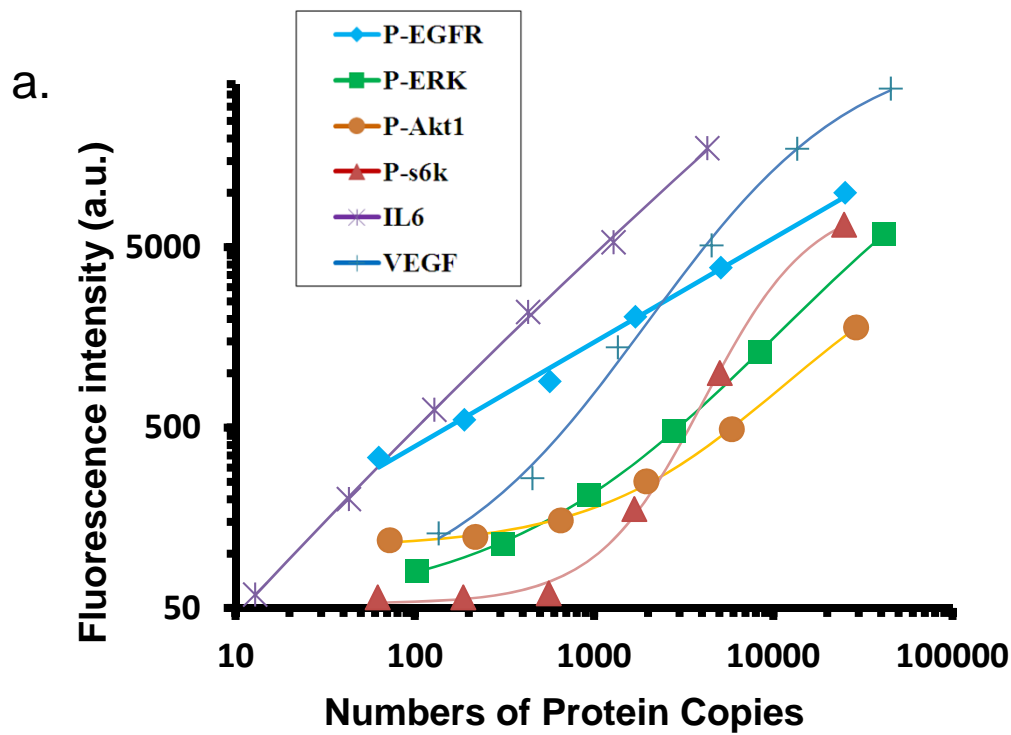


Figure S4. Calibration and Cross-reactivity analysis of antibody arrays. **a.** Calibration curves of P-EGFR, P-ERK, P-mTOR, P-Akt1, P-s6k, IL6 and VEGF using recombinant proteins. The number of copies of each protein in a microchamber is calculated by from the concentration of the stock solution within the 0.144 nanoliter volume of the microchamber. These calibration curves were measured on an SCBC that was identical to those used for the experiments. **b.** Cross-reactivity characterization of P-EGFR, P-ERK, P-mTOR, P-Akt1 and P-s6k. The ssDNA barcode array was printed using a standard DNA spotting system, but the ELISA-like immunoassays used for these studies were identical to those used in the experiments. Cross-reactivity was <2% for all proteins in the panel.

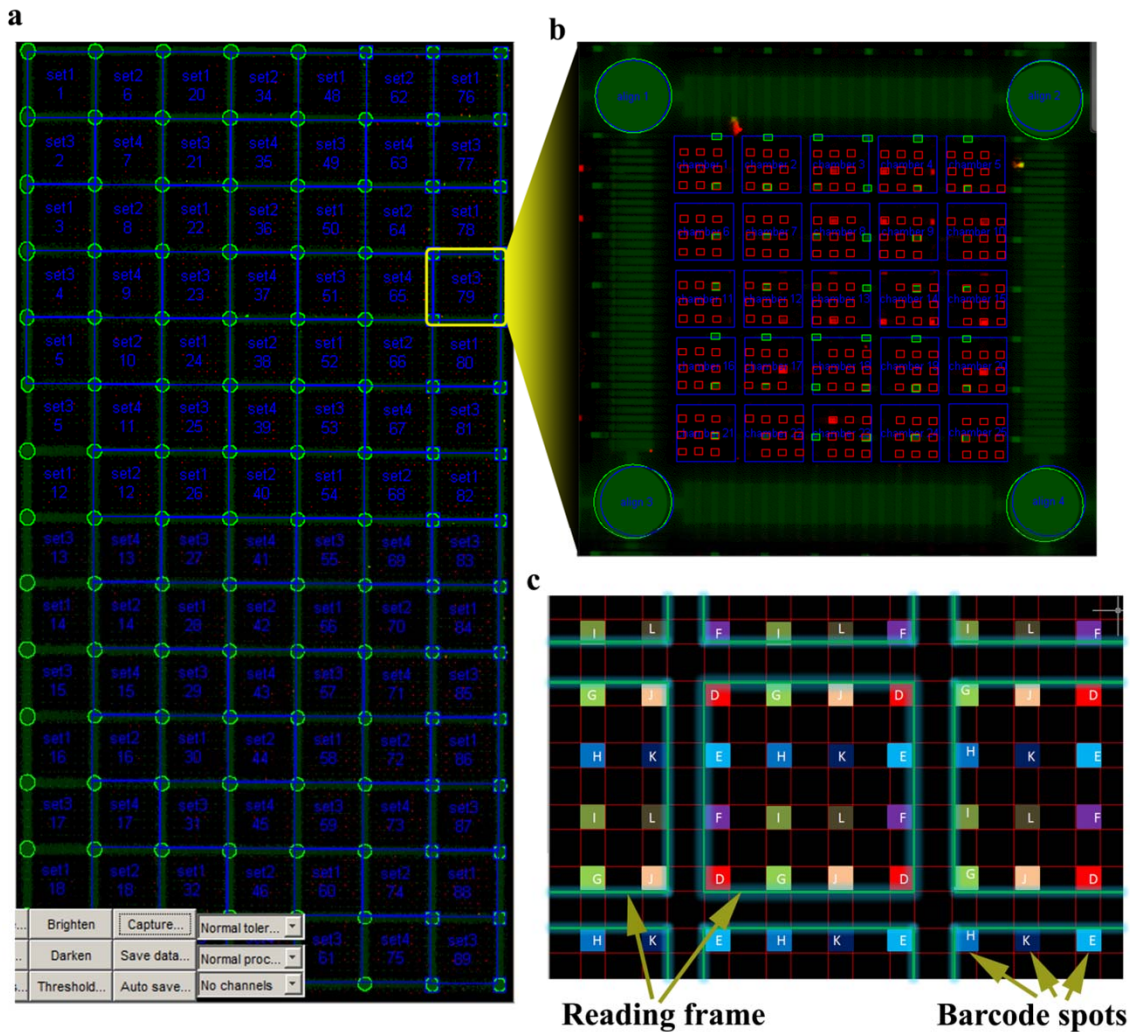
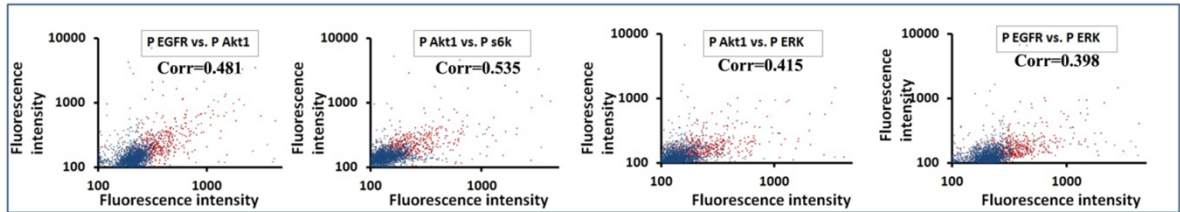
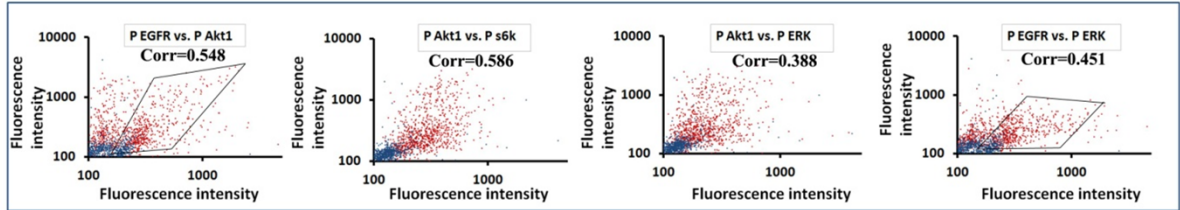


Figure S5. Reading of a developed SCBC assay and automation of data processing. (a) The glass slide of an SCBC was scanned with an array scanner to extract the fluorescence intensity of the spots within each antibody array. The data shown here is visualized by an overlay image that was generated by a laboratory developed Matlab program. Each square outlined region is a lattice unit, and each lattice unit contains between 20 and 25 cell microchambers (depending upon whether the SCBC was designed for cell lysis or not). (b) A single lattice unit, showing the actual fluorescence image of the developed protein assays from 25 microchambers. The array spots designated as alignment markers show up as green fluorescent squares. (c) The alignment markers are used to assign protein identities to each array element. The program identifies each cell chamber as a reading frame, and assigns the protein identity to each spot of a barcode. Note that some proteins are assayed in duplicate.

a U87 cells



b U87 cells + EGF



c U87 VIII cells

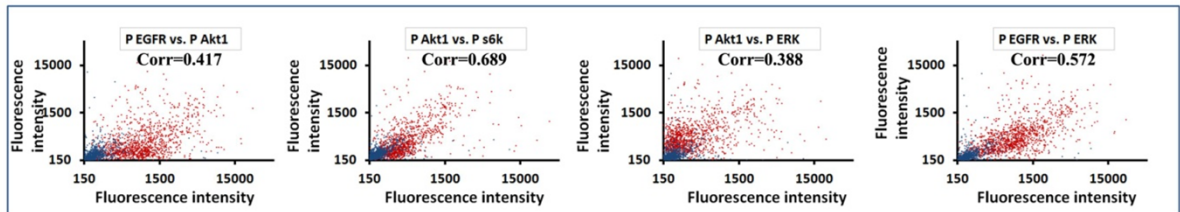


Figure S6. Scatter plots showing fluorescent levels and correlations of the assayed phosphoproteins from an SCBC measurement for two model GBM cell lines. Data from 0 cell (blue) and 1 cell (red) are superimposed to illustrate the baseline level. The samples used in this study are U87 cells (a), U87 cells stimulated with EGF (b) and U87 EGFRvIII cells (c). For each plot, the correlation coefficient between two phosphoproteins is provided. The U87 cells are not constitutively activated, and so their phosphoprotein levels are expected to be less than those seen for the U87 EGFRvIII cells. EGF stimulation of the U87 cells activates those cells, and is expected to increase the levels of the assayed phospho-proteins.

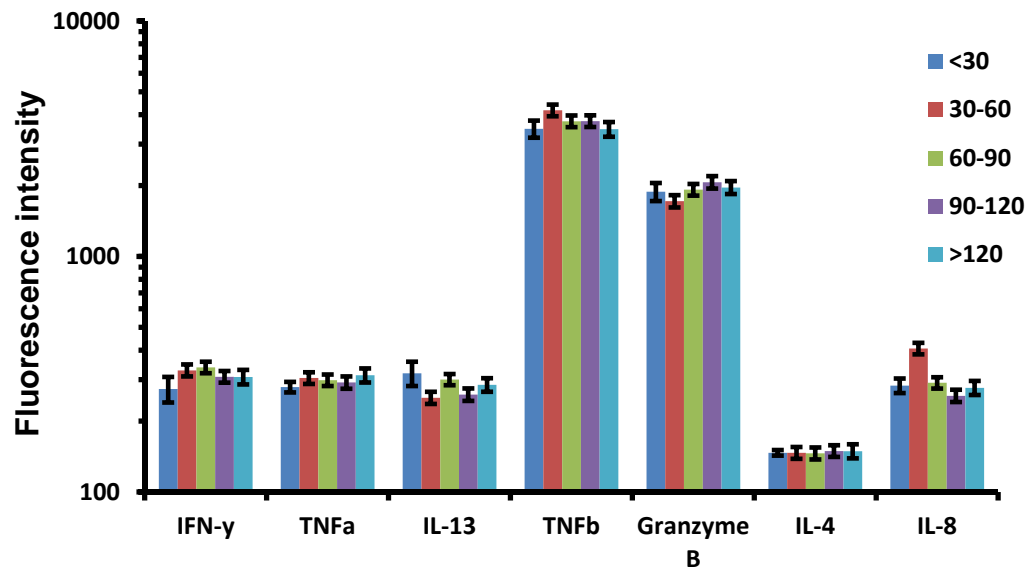


Figure S7. Results of a control experiment in which the levels of the indicated secreted proteins were assayed from T cells following a 6 hour incubation time. These non-adherent cells were screened from a healthy donor. They could move around during the course of the incubation. Thus, even if the cells interact in a distance dependent fashion so as to influence the levels of these assayed proteins, that influence would be expected to be washed out. Thus, no distance-dependence in the protein levels is expected, and non is observed.

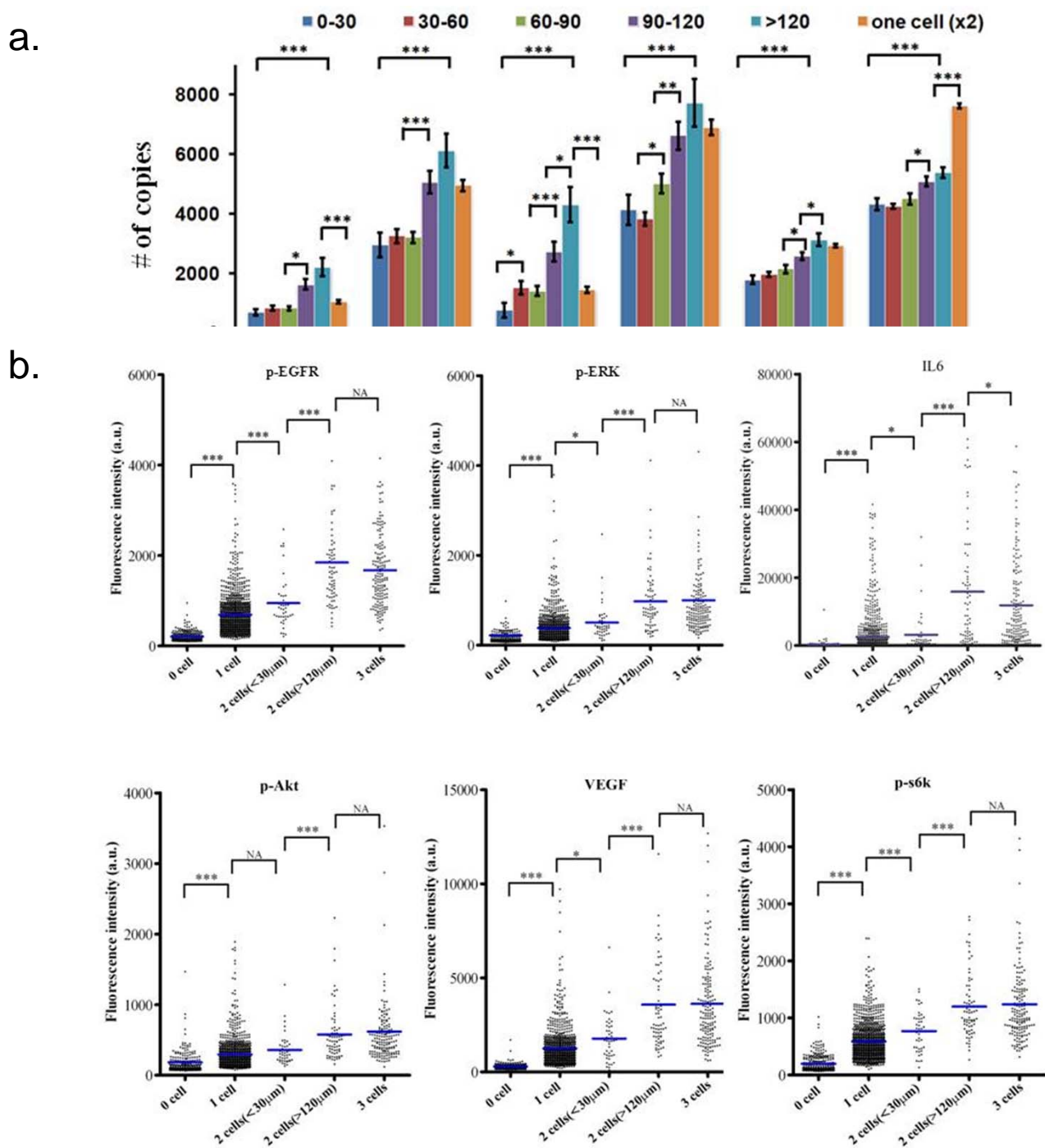
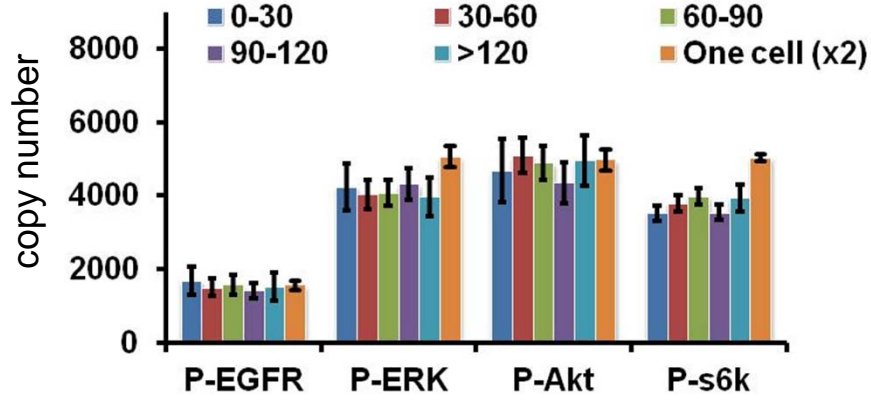


Figure S8. Statistical analysis of SCBC data, 6 hour incubation experiment. **a.** Average values of protein levels for 1- and 2-cell experiments. The 2-cell experiments are given as a function of cell separation. Calculated P -values are indicated. **b.** Dot plot of 0-, 1-, 2-, and 3-cell data sets for each assayed protein. The 2-cell data sets that represent the smallest and largest cell-cell separations are shown. All data are from the same SCBC; the 0-cell data represent an empty microchamber, and so provide a background measurement. The blue bar indicates the mean protein level at each condition. For both plots, P values are 0.05 (*), 0.01 (**), and 0.001 (***), with 0.05 considered statistically significant. An insignificant statistical difference ($P > 0.05$) is denoted as NA.

a.



b.

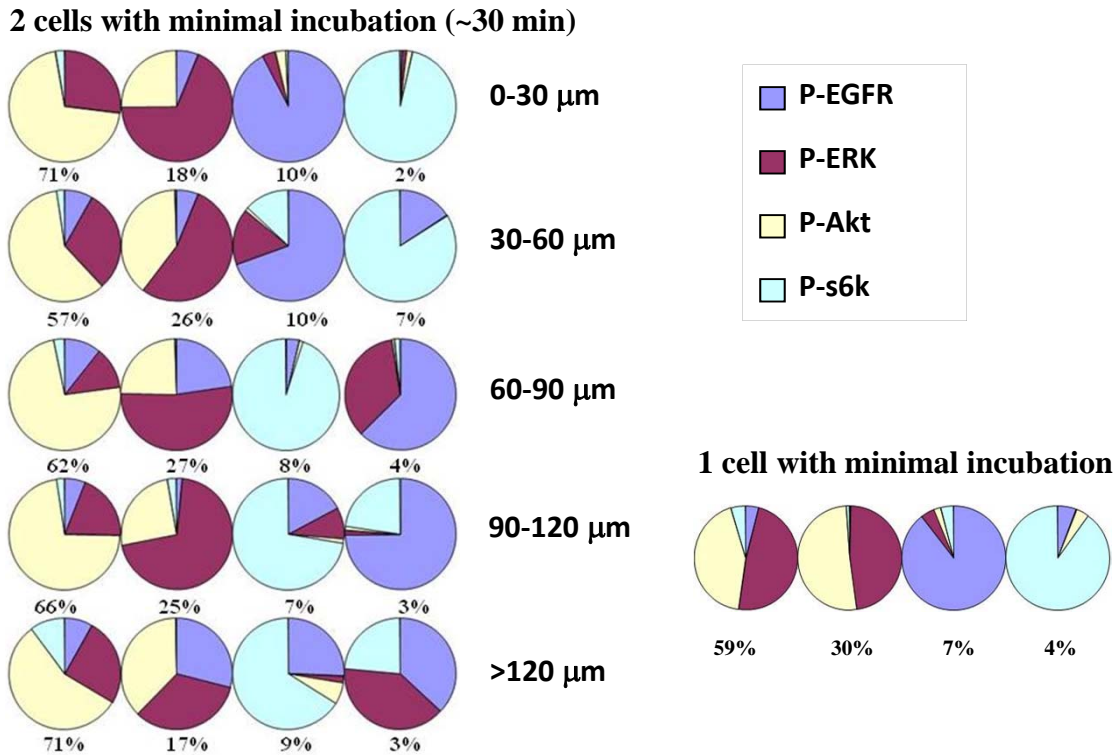


Figure S9. Data from the minimal incubation time experiment. **a.** Average protein levels, in copy numbers, as a function of cell-cell distance in the 2-cell experiments. The average single-cell value ($\times 2$) is provided for comparison. **b.** Coordination of the 4 phospho-proteins for the 1-cell and cell separation dependent 2-cell experiments. The pie charts represent the eigenvector compositions; all 4 eigenvectors are shown, with eigenvalues given as relative amplitudes (in %). No obvious change of coordination is found for the various cell separations, or between the 1 cell and 2 cell experiments. Secreted proteins are not detected in these assays.

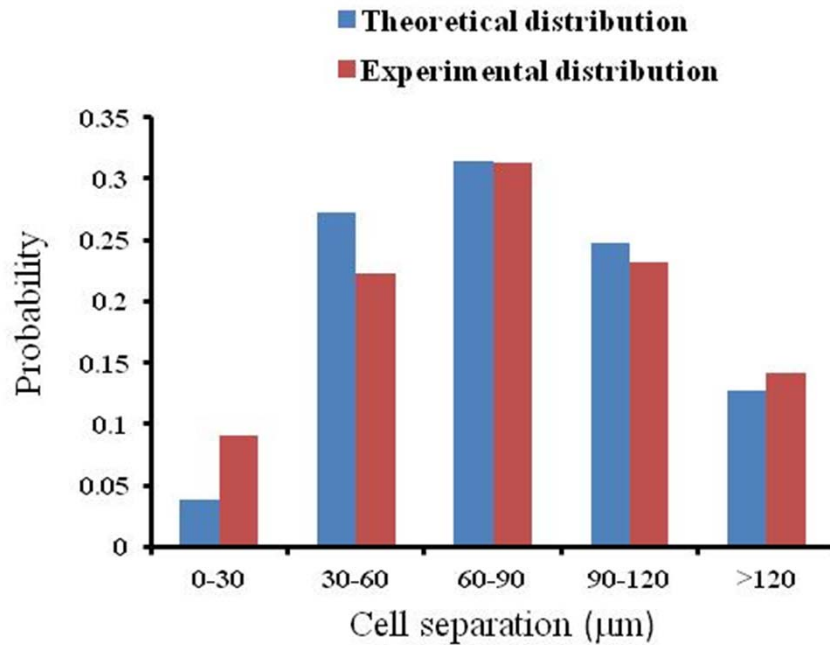


Figure S10. A histogram of the observation frequency of the experimentally measured cell separation distances (6 hour incubation experiment), compared against a simulated distribution generated by placing cells in random positions. A custom Matlab program was used to randomly generate ~90,000 cell pairs, and to calculate cell-cell distances. The simulation conditions were that the cells were wholly located within the same microchamber, and that they don't overlap. The agreement between the simulation and the experiment indicates that the inhibitory and activating interactions measured at the functional protein level do not translate into attractions and repulsions that can influence cell-cell separation distance, at least on the 6 hour timescale of the experiment.

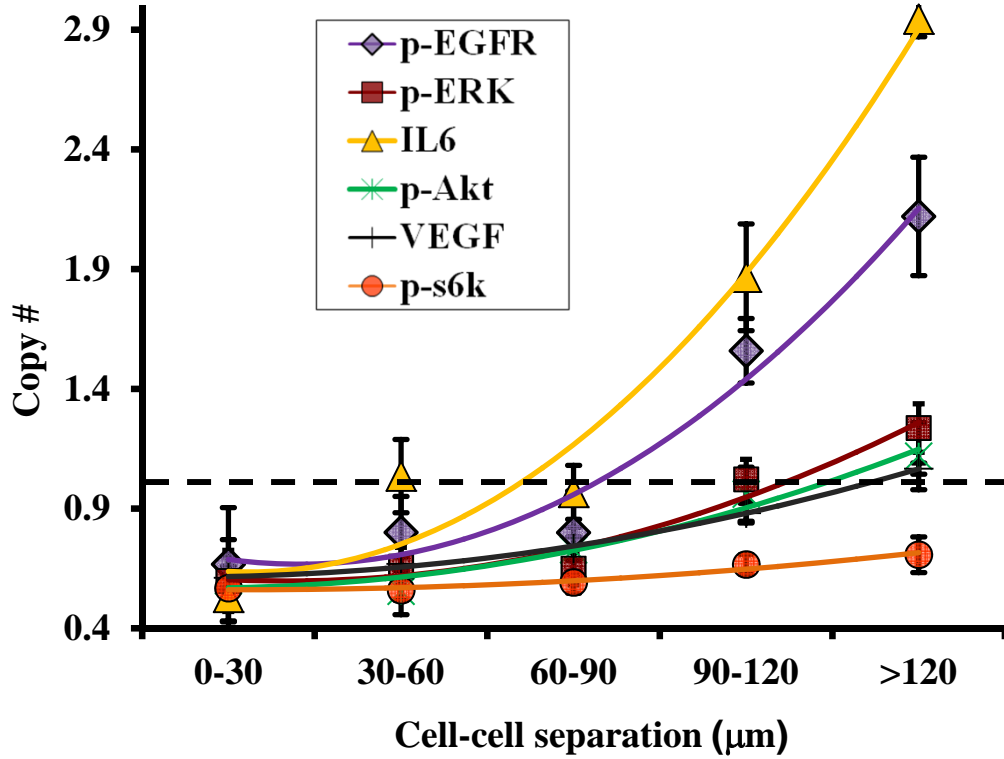


Figure S11. Protein-specific cell-cell interaction functions. These functions are obtained by fitting the measured protein level vs separation distance to the quadratic equation

$$f(L_{AB}) = a + b \cdot L_{AB} + c \cdot L_{AB}^2, \text{ where } a, b, \text{ and } c \text{ are fitted constants, and } L_{AB} \text{ is the cell-cell distance.}$$

The protein copy numbers are from the 6 hour incubation, 2-cell experiments, and are normalized to 2x the average single cell experimental value (horizontal dashed line).

Supporting Tables

Table S1. Sequences of ssDNA oligomers and terminal functionalization.*

Name	Sequence**
2X A-3'-polyA	ATCCTGGAGCTAAGTCCGTAAAAAAAAAAAAAAAAAAAAAAAAAATCCTGGAGCTAAGTCCGTAAAAAAAAAAAAAAAAAAAAAAAAA
2X B-3'-polyA	GCCTCATTGAATCATGCCTAAAAAAAAAAAAAAAAAAAAAAAAAGCCTCATTGAATCATGCCTAAAAAAAAAAAAAAAAAAAAAAAA
2X C-3'-polyA	GCACCTCGTCTACTATCGCTAAAAAAAAAAAAAAAAAAAAAAAAAGCCTCGTCTACTATCGCTAAAAAAAAAAAAAAAAAAAAAAAA
A'-D-D	ATGGTCGAGATGTCAGAGTAAAAAAAAATGGTCGAGATGTCAGAGTAAAAAAAAATACGGACTTAGCTCCAGGAT
D3'	NH ₂ -AAAAAAAAAAAAAAAAA TACTCTGACATCTCGACCAT
B'-E-E	ATGTGAAGTGCGAGTATCTAAAAAAAAATGTGAAGTGCGAGTATCTAAAAAAAAATAGGCATGATTCAATGAGGC
E3'	NH ₂ -AAAAAAAAAAAAAAAAA TAGATACTGCCACTTCACAT
C'-F-F	ATCAGGTAAGGTTACGGTAAAAAAAAATCAGGTAAGGTTACGGTAAAAAAAAATAGCGATAGTAGACGAGTGC
F3'	NH ₂ -AAAAAAAAAAAAAAAAA TACCGTGAACCTTACCTGAT
A'-G-G	GAGTAGCCTTCCCGAGCATTAAAAAAAAAGAGTAGCCTTCCCGAGCATTAAAAAAAAATACGGACTTAGCTCCAGGAT
G'	NH ₂ -AAAAAAAAAAAAAAAAA TGCTCGGGAAGGCTACTC
B'-H-H	ATTGACCAAACGCGGTGCGAAAAAAAAATTGACCAAACGCGGTGCGAAAAAAAAATAGGCATGATTCAATGAGGC
H'	NH ₂ -AAAAAAAAAAAAAAAAA ACGCACCGCAGTTTGGTCAAT
C'-I-I	TGCCCTATTGTTGCGTCGGAAAAAAAAATTGCCCTATTGTTGCGTCGGAAAAAAAAATAGCGATAGTAGACGAGTGC
I'	NH ₂ -AAAAAAAAAAAAAAAAA TCCGACGCAACAATAGGGCA
A'-J-J	TCTTCTAGTTGTCGAGCAGGAAAAAAAAATCTTCTAGTTGTCGAGCAGGAAAAAAAAATACGGACTTAGCTCCAGGAT
J'	NH ₂ -AAAAAAAAAAAAAAAAA CTTGCTCGACAACACTAGAAGA
B'-K-K	TAATCTAATTCTGGTCGCGAAAAAAAAATAATCTAATTCTGGTCGCGAAAAAAAAATAGGCATGATTCAATGAGGC
K'	NH ₂ -AAAAAAAAAAAAAAAAA ACCGCGACCAGAAATTAGATTA
C'-L-L	GTGATTAAGTCTGCTTCGGAAAAAAAAAGTGATTAAGTCTGCTTCGGAAAAAAAAATAGCGATAGTAGACGAGTGC
L'	NH ₂ -AAAAAAAAAAAAAAAAA GCCGAAGCAGACTTAATCAC

* All oligonucleotides were synthesized by Integrated DNA Technology (IDT) and purified via high performance liquid chromatography (HPLC).

** Purple color sequences are anchored to the glass surface as the first layer of the ssDNA array. Red color sequences are bridging sequences to the complementary purple color sequences. The blue color sequences are used to conjugate DNA-labeled antibodies.

Table S2. List of antibodies used for GBM cell proteomic assay.

DNA label	Antibody (vendor: clone)	Source
D	mouse anti-hu phospho-EGF R biotin-labeled goat anti-hu EGF R	R&D Y1068 R&D BAF231
E	anti-hu phospho-ERK kit	R&D DYC1825
F	anti-IL 6 kit	R&D DYC206
G	anti-hu phospho-mTOR kit	R&D DYC1665
I	anti-hu phospho-Akt1 kit	R&D DYC2289
K	anti-VEGF kit	R&D DYC293B
L	anti-hu p70 s6 kinase	R&D DYC896

Table S3. Protein-protein correlation coefficients in EGFRvIII cells for varying incubation times and cell-cell separation distances. All measurements from 2-cell assays and from molecule copy number.

Table S3a. 6 hour incubation, 0-30 μm separation

	P-EGFR	P-ERK	IL6	P-Akt	VEGF	P-s6k
P-EGFR	1.00	0.72	0.45	0.66	0.50	0.63
P-ERK		1.00	0.49	0.72	0.63	0.67
IL6			1.00	0.43	0.49	0.31
P-Akt				1.00	0.62	0.70
VEGF					1.00	0.74
P-s6k						1.00

Table S3b. 6 hour incubation, >120 μm separation

>120 μm	P-EGFR	P-ERK	IL6	P-Akt	VEGF	P-s6k
P-EGFR	1.00	0.81	0.67	0.63	0.64	0.62
P-ERK		1.00	0.77	0.73	0.74	0.67
IL6			1.00	0.53	0.52	0.44
P-Akt				1.00	0.73	0.74
VEGF					1.00	0.77
P-s6k						1.00

Table S3d. 30 min incubation, 0-30 μm separation

0-30 μm	P-EGFR	P-ERK	P-Akt	P-s6k
P-EGFR	1.00	0.09	0.11	0.21
P-ERK		1.00	0.39	0.26
P-Akt			1.00	0.47
P-s6k				1.00

Table S3e. 30 min incubation, >120 μm separation

	P-EGFR	P-ERK	P-Akt	P-s6k
P-EGFR	1.00	0.52	0.29	0.30
P-ERK		1.00	0.21	0.28
P-Akt			1.00	0.45
P-s6k				1.00

Supporting Materials and Methods

General microchip fabrication steps. Microchips were used for antibody array flow patterning and for the single cell barcode chips. For both, standard photolithographic techniques were used to prepare a hard mold from which the elastomer component of the final microchip was cast. To this purpose, 5” chrome lithography masks were designed with AutoCAD 2007 (Autodesk Inc.) and printed out by UCLA Nanolab foundry. The features on the chrome mask were used to pattern SU8 and/or SPR220 photoresist on a 4” silicon wafer. For the flow patterning molds, the photoresist thickness, which translates into the height of the flow channels, was 25 μm . For the SCBC chips, multiple masking steps using two different photoresists produced a mold with three-dimensional structure, as shown in Figure S1.

Antibody array preparation. The approach for antibody array preparation was previously used for the high resolution patterning of cells and tissues.¹ It is used here for the preparation of miniature 3×3 antibody arrays for protein capture. The arrays are initially patterned as DNA arrays, since DNA has the physical and chemical stability to withstand the various processing steps of microfluidics fabrication. The DNA itself is patterned onto a polylysine coated glass slide using two sequential microchannel-based flow patterning steps (Figure S2). The first flow patterning step generates 20 μm wide, 50 μm pitch lines of 3 unique DNA oligomers, while the second DNA patterning step, using a similarly structured mold, is carried out at right angles to the first. The actual antibody array is formed at the intersection of the two sets of lines. Substantially smaller and denser features are possible with this approach.¹ The trick is to choose the right sets of DNA oligomers in the two patterning steps so that, at the intersection of 3 bottom lines and 3 top lines, a 9 element array of uniquely addressable ssDNA oligomers is formed. Those unique addresses are then used as assembly locations for antibodies that have been labeled with complementary ssDNA’ oligomers. All DNA and antibody reagents used are provided in Supporting Tables S1 and S2.

For the first flow patterning step, a PDMS mold containing 20 channels was used to flow pattern three distinct 80-mer ssDNA “anchor” strands (**A**, **B**, **C**; 266 μM in 33% DMSO) in adjacent sets of three channels (one distinct strand per channel), to produce 6 2/3 complete sets of lines (Figure S2). The microchip was then incubated in a humidified environment for one day, before exposure to 2.5 mW UV light for 5 min to crosslink the DNA/polylysine film. The chip is then incubated at room temperature for 1 day and the glass slide was separated from the PDMS. The surface was and rinsed sequentially with 0.02% SDS in PBS (2×), followed by PBS and deionized (DI) water. The slide was dried under flowing N_2 .

A second microfluidics flow patterning step was then carried out at right angles to the first. Again, a 20 channel mold was used, making up 6 2/3 repeats of 3 adjacent microchannels that carried distinct DNA solutions - in this case, each solution was comprised of three distinct ssDNA “bridge” oligomers (**A’-i**, **B’-ii**, ...). Each bridge oligomer includes a 20-base pair tail that is complementary to one of the three anchor sequences, and a 20-base pair head with a

unique sequence. As such, once the flow-patterning was complete, the resultant 3×3 arrays (Figure S3) contained nine spatially addressable oligonucleotide head sequences (i–ix) that were available to bind distinct capture antibodies conjugated to one of nine complementary ssDNA strands (i'–ix'). For this patterning step, three patterning solutions were constructed from 3 separate 150 μ M DNA solutions in 1% BSA. Solutions were infused into the microchannels. The microchip was incubated for 2 hours to allow the arrays to assemble via DNA hybridization, followed by injection of 3% PBS/BSA to wash out residual DNA in microchannels. The microchip was disassembled, and a rinsing procedure identical to that for the first flow patterning step was used. The patterned slides were preserved in a desiccator for no more than 2 month.

DNA array validation. The patterned DNA array was validated by first blocking it with 3% bovine serum albumin (BSA) in PBS for 1 h at room temperature. The blocking reagent was replaced by 100 nM cy5 conjugated complementary DNA oligomers, and the slide was incubated for another hour at 37 °C. The slide was rinsed with 3% BSA in PBS twice and DI water, and dried under flowing N₂. It was then scanned by a Genepix scanner (Molecular Devices, LLC.) (Figure S3). The validation procedure provides a check on the cross-reactivity between the anchor, bridging, and terminal ssDNA oligomers. In addition, the fluorescence intensity per unit area can be compared against standard DNA spotting approaches as a means of gauging surface coverage. Finally, it provides an assessment of the fidelity of the microfluidics flow-patterning steps.

Antibody array calibration and cross reactivity characterizations. Procedures for calibration and cross-reactivity characterizations of our barcode assays have been described before^{1, 2}. We used recombinant IL6, VEGF, p-EGFR, p-ERK, p-Akt and p-s6k and p-mTOR proteins (R&D Systems, Inc.) at various concentrations (Figure S4a) to calibrate the fluorescence intensity of a barcode assay with molecule number in a cell chamber with a volume of 0.144 nl. These calibrations were executed in a fashion identical to a standard SCBC experiment, except that the recombinant protein solutions were added in place of the cells. Antibody cross-reactivity assays (Figure S4b) were carried out using arrays comprised of identical biomolecular reagents, but prepared via spotting procedures, rather than through flow patterning. All antibody reagents used are listed in Table S2.

SCBC fabrication. The SCBC chip is a single elastomer microfluidics layer bonded on top of the barcode-patterned glass slide. The elastomeric layer mold was patterned in several steps. A side view that shows the essential patterned features for structural support, cell microchambers, and microchannels, is shown in Figure S1. The cell microchambers are designed so that their volume is minimized. Each microchamber is $170 \times 170 \mu\text{m}$, and 16 μm high.

Cell sample preparation. U87 cells were purchased from American Tissue Culture Collection (ATCC). U87 EGFRvIII cells were constructed as reported^{3, 4}. The cells were cultured in DMEM (ATCC) medium supplemented with 10% fetal bovine serum (FBS) in a 5% CO₂ incubator at 37 °C. Cells were trypsinized and subcultured every two days. Cells were concentrated to

1×10^5 /ml in a volume of at least 100 μ l. To facilitate cell imaging and counting, cells were stained with 5 μ M CMFDA in PBS for 10 min, and re-suspended with a desired concentration. Cell viability, estimated at 95%, was confirmed by visual inspection of the cells within the chambers, since the live U87 EGFRvIII cells spread out and retaining the CMFDA dye within their membrane.

SCBC operation. The mating surface of a molded PDMS layer for the single cell barcode microchip was rendered hydrophilic by an O₂ plasma etcher (Quorum Technologies Ltd.), and aligned by eye and mated onto a barcoded glass slide. Such imprecise alignment is effective because the DNA barcode arrays are patterned at such high density, relative to the size of the microchambers, that each microchamber is ensured of overlapping with at least one complete barcode. The microchannels were blocked with 3% BSA in PBS for 1 h, and filled with 10 μ g/ml antibody-DNA conjugates (Table S2).⁵ After incubation at 37 °C for 1 h, unlinked conjugates were washed off and replaced by 3% BSA in PBS. At the point, the ssDNA array has been transformed into an antibody array. The SCBC is then mounted onto a clamp (Figure 1b). Cells at a concentration of 1×10^6 per ml were loaded onto the microchip by pipetting through the inlet ports on the SCBC, with no pressure from the clamp. Then cells were distributed randomly to the microchambers. Pressure was then adjusted to encapsulate cells within the microchambers (Close I and II states are both sufficient).

After the U87 EGFRvIII cells were loaded to the SCBC, the clamp pressure was adjusted to the Close II state (Figure 1b). For the minimal incubation time experiment, we imaged all cell chambers using a fluorescence microscope. That process took 30 minutes. Then a 3 \times lysis buffer (20 mM Tris-HCl, 150 mM NaCl, 1 mM Na₂EDTA, 1 mM EGTA, 1% Triton, 2.5 mM sodium pyrophosphate, 1 mM β -glycerophosphate, 1 mM Na₃VO₄, and 1 μ g/ml leupeptin; Cell Signaling) supplemented with protease/phosphatase inhibitor cocktail (Cell Signaling) was injected into the microchannels, and the clamp was adjusted to the Close I state, which permits introduction of lysis buffer into each cell chamber, but doesn't permit cell escape. The SCBC was incubated at room temperature with mild shaking for 2 h. The lysis buffer was then removed by flowing PBS for 15 min.

For the 6 hr incubation experiments, cells were loaded and the clamp was adjusted to the Close II state, after which the clamped SCBC was incubated at 37 °C for 6 h in a CO₂ incubator. Then all cell chambers were imaged using a fluorescence microscope, and the remaining steps were identical to those described for the minimal incubation time experiment.

In order to localize the position of each unit of microchambers, a staining solution containing 20 μ M Alexa 514 succinimidyl ester (Molecular Probes, Inc.) was used to label microchannels for 10 min under the Close II state. Dye residue was removed by injecting 3% BSA in PBS and incubated for 20 min. The clamp was then release to form the open state, and biotinylated detection antibody (R&D systems, Cell signaling) cocktails in 1:200 dilution prepared according to product instruction was injected into the microchannels. After a 2 hr incubation with mild

shaking, the antibody solution was cleaned by 3% BSA in PBS, and a solution comprised of 1 μ M cy5-Streptavidin and 100 nM H-cy3 in PBS with 3% BSA was used to develop the barcode arrays. The glass slide containing the developed arrays was detached from the PDMS, and cleaned for further scanning.

Assay quantification and statistics. Developed barcode slides were scanned with an Axon GenePix 4400A (Molecular Devices) with setting of: (for cy5 dye, 635 nm) laser power 80%, optical gain 600; (for cy3 dye, 532 nm) laser power 15%, optical gain 450 for 532 nm. The resultant images were digitized at 16 bits (scale of 0-65535). For data analysis, the GenePix Pro software exported the digitized fluorescence image to a custom algorithm, written in Matlab (MathWorks, Inc.), that automated the process (Figure S5) of associating the individual array spots with microchamber address labels and protein identification tags.

Statistical analysis was performed using laboratory developed Matlab (Mathworks) programs and Prism (GraphPad Software). To compare protein levels under various conditions, we obtained the mean protein number, and used P value to evaluate the whether the difference was significant through two-tailed Student's t tests assuming unequal variance. A P value less than 0.05% is considered statistically significant and denoted with *, while ** and *** represent $P < 0.01$ and $P < 0.001$, respectively. The error bars for mean protein levels represent the standard error of the mean, which is the standard deviation of the mean protein level divided by square root of cell number. This type of analysis was carried out to establish the statistical uniqueness of the 0, 1, 2, and 3 cell data sets, as well as the uniqueness of the different 2 cell data sets, as a function of cell-cell separation (Figure S6).

Signaling coordination analysis. For a given set of experimental conditions (e.g. 2 cells, 6 hour incubation, 30-60 μ m separation) the corresponding protein assays were converted into copy numbers detected, and the protein-protein covariance matrix was calculated and diagonalized using Matlab functions. This yielded 6 eigenvectors and 6 eigenvalues (Figure 2 and Figure S8).

Two-cell distribution simulations. We simulated the placement of the cells in 2-cell experiments to interrogate whether their locations were influenced through the inhibitory or activating interactions. An elliptic shaped cell of dimensions $25 \mu\text{m} \times 7.5 \mu\text{m}$ provided a mimic of the adherent U87 cells. The program randomly sets the position of the first cell, and then generates the second cell in a random position, with the conditions that both cells are within the same microchamber, and the cells do not overlap. We simulated 90,000 cell pairs, and then measured the distances between the cells, from cell-center to cell-center. These distances were binned into 5 groups, and compared with experimental result (Figure S9).

Simulations of protein levels from 3-cell microchamber experiments. For these simulations, we first fitted the 6 hour incubation, two-cell microchamber data of Figure 2a to $f(L_{AB}) = a + bL_{AB} + cL_{AB}^2$, where a , b and c are protein-specific fitted constants and L is the cell-cell distance. Those fits are provided in Figure S10. The plotted data is normalized by the

average value for that protein from the one-cell experiments (the dashed, horizontal line of Figure S10).

A custom written Matlab program was written for simulating 3-cell experiments. Each cell was modeled as a 25 μm x 7.5 μm ellipse to provide a mimic of an adherent cell. Three cells were randomly placed within a microchamber, with the conditions of zero cell-cell overlap, and that each cell was fully contained within the microchamber walls. The program generated ~12,000 three cell data sets, and computed the distances between each cell pair, using the center of the ellipse to define the cell location. The algorithm for calculating individual protein levels was:

- a.** The protein levels for each of the three cells, A, B, and C, are initially set to the corresponding average from the single cell experiments. This is the y-axis value of '1' on Figure S10.
- b.** Based upon the fitted protein-specific distance functions, the pairwise interactions for A-B, B-C, and C-A are calculated. As an example, from Figure S10, if A-B are separated by 40 μm , then p-EGFR is inhibited by a factor of 0.69 for each cell. If A-C are separated by 90 μm , then p-EGFR is activated by a factor of 1.17. Multiplying these two factors together gives the normalized amount of p-EGFR for A (=0.81). Next this procedure is repeated for cell B and lastly for cell C. The amount of protein estimated for this 3-cell experiment is the sum over all 3 cells. The result is independent of which cells are labeled A, B and C. This procedure is done for each protein, and for each one the result is averaged for all ~12,000 simulated 3-cell experiments to produce the predictions of Figure 3.

References

- (1) Ma, C.; Fan, R.; Ahmad, H.; Shi, Q. H.; Comin-Anduix, B.; Chodon, T.; Koya, R. C.; Liu, C. C.; Kwong, G. A.; Radu, C. G.; Ribas, A.; Heath, J. R. *Nat. Med.* **2011**, 17, (6), 738-U133.
- (2) Shi, Q. H.; Qin, L. D.; Wei, W.; Geng, F.; Fan, R.; Shin, Y. S.; Guo, D. L.; Hood, L.; Mischel, P. S.; Heath, J. R. *Proc. Natl. Acad. Sci. USA* **2012**, 109, (2), 419-424.
- (3) Mellinghoff, I. K.; Wang, M. Y.; Vivanco, I.; Haas-Kogan, D. A.; Zhu, S. J.; Dia, E. Q.; Lu, K. V.; Yoshimoto, K.; Huang, J. H. Y.; Chute, D. J.; Riggs, B. L.; Horvath, S.; Liau, L. M.; Cavenee, W. K.; Rao, P. N.; Beroukhi, R.; Peck, T. C.; Lee, J. C.; Sellers, W. R.; Stokoe, D.; Prados, M.; Cloughesy, T. F.; Sawyers, C. L.; Mischel, P. S. *New Engl. J. Med.* **2005**, 353, (19), 2012-2024.
- (4) Wang, M. Y.; Lu, K. V.; Zhu, S. J.; Dia, E. Q.; Vivanco, I.; Shackleford, G. M.; Cavenee, W. K.; Mellinghoff, I. K.; Cloughesy, T. F.; Sawyers, C. L.; Mischel, P. S. *Cancer Res.* **2006**, 66, (16), 7864-7869.
- (5) Bailey, R. C.; Kwong, G. A.; Radu, C. G.; Witte, O. N.; Heath, J. R. *J. Am. Chem. Soc.* **2007**, 129, (7), 1959-1967.